IEEE Access
Multidisciplinary | Rapid Review | Open Access Journal

Received March 24, 2019, accepted April 13, 2019, date of publication April 17, 2019, date of current version April 29, 2019.

Digital Object Identifier 10.1109/ACCESS.2019.2911665

Decentralized Adaptive Under Frequency Load Shedding Scheme Based on Load Information

PEICAN HE, BUYING WEN, AND HUAIYUAN WANG
Fujian Key Laboratory of New Energy Generation and Power Conversion, College of Electrical Engineering and Automation, Fuzhou University, Fuzhou 350108, China

Corresponding author: Huaiyuan Wang (79749544@qq.com)

ABSTRACT The inertia of the power system changes when the generators in the system are disturbed or tripped. However, in some systems, there is no control center or communication device falling behind. It makes real-time inertia difficult to obtain and affects the adaptive under frequency load shedding (UFLS) scheme. This paper proposes an adaptive decentralized UFLS scheme based on load information to overcome this problem. First, a calculation method is derived according to the load information after the disturbance to identify the real-time of load equivalent virtual inertia. Then, the power deficit of load is estimated and the optimal adaptive load shedding scheme is obtained. Finally, compared with conventional UFLS schemes, the proposed scheme can be performed merely by load information. Hence, the requirement of communication conditions and the dependence on the control center are reduced. The simulation is carried out on the island utilizing the IEEE39-bus system. Furthermore, the accuracy of real-time identification of load equivalent virtual inertia and the validity of the load shedding scheme are verified.

INDEX TERMS Load information, power deficit, inertia calculation, frequency stability, real-time calculation.

I. INTRODUCTION

Frequency stability is an essential challenge to maintain the power system performance. Therefore, frequency is important to be maintained within the allowable range of deviation [1], [2]. The fixed UFLS device can be applied to keep the rated value of frequency during occurrence of the system frequency stability problem [3], [4]. The parameters of the traditional UFLS are obtained through an offline simulation. However, the variety of system operating conditions and potential disturbances in actuality lead to inexhaustible possible scenarios. Meanwhile, the simulation models and parameters are difficult to be extracted from the actual system due to the complexity of load components and the diversity of generator parameters. The validity of traditional UFLS depends on the similarity between the anticipated accident and the actual fault. Therefore, the applicability of UFLS with preset parameters is limited.

The wide area measurement system (WAMS) is built on the basis of phasor measurement units (PMUs) and communication technology. The real-time operating information obtained by WMAS can be applied to monitor the operation state of power systems [5], [6]. Moreover, the essential conditions for stability control technologies based on response information of power systems are provided. According to the frequency response model, the relationship between the rate of change of frequency (RoCoF) of the inertia center and unbalanced power is derived [7], [8]. And the proportional coefficient is the equivalent inertia of power systems. This proportional relation becomes the core algorithm of the adaptive UFLS schemes [7], [9]–[11].

There are many adaptive improvements of UFLS methods. The main research progress in UFLS includes the following aspects. One aspect is mainly based on response information. Among them, transforming the UFLS problems into optimization problems can determine the optimal load shedding by particle swarm optimization (PSO) [12]. Lately, the frequency threshold of load shedding relays is adaptively tuned at each disturbance [13], [14], but this approach lacks an effective estimation of the power deficit. Hence, a dynamic correction method for the power deficit is proposed [15]. But multiple rounds of actions are also required to approach the power deficit. And the other aspect is on the basis of prediction information. The predictive method is an important aspect on possible UFLS protection. The second derivative of frequency is proposed to forecast the value of the

The associate editor coordinating the review of this manuscript and approving it for publication was Sofana Reka S.

frequency minimum. And actual load shedding control can be guided according to the predictive frequency [11], [16]. Moreover, an adaptive UFLS scheme based on the minimum frequency prediction is presented [17], and the randomness of renewable energy generation is also taken into account. It ensures the recovery of frequency while the load shedding amount is reduced effectively.

There are two ways to realize UFLS: centralized control and decentralized control. If the centralized adaptive UFLS is adopted, a control center and a two-way communication network need to be established. The system inertia and RoCoF can be achieved through the decentralized measuring devices [4], [18], [19]. This puts forward high requirements for the real-time capability, synchronicity, and reliability of communication networks.

If the decentralized adaptive UFLS is adopted, the requirement of UFLS schemes on communication conditions and the dependence on the control center are greatly reduced. Generally, system inertia is presupposed [20], [21]. However, it may change greatly when a disturbance occurs. The control validity will inevitably be affected by the fixed system inertia. Thus, an adaptive inertia calculation method is important for the UFLS schemes.

A decentralized UFLS scheme based on load information is proposed in this paper. Firstly, under the premise of no unified control center, the decentralized equivalent virtual inertia is derived according to the load information. And then, the power deficit of load can be estimated based on equivalent virtual inertia. Finally, a decentralized adaptive UFLS scheme can be acquired. The dependence on the control center and communication network is reduced in UFLS schemes. And it can be better adapted to various disturbances that may occur in the system. Frequency stability is significantly improved by the proposed UFLS scheme.

II. INERTIA ESTIMATION BASED LOAD INFORMATION

The rotor motion equation of a generator is described as follows:

$$M\frac{d\Delta\omega}{dt} = P_m - P_e - D\Delta\omega = -\Delta P\ , \tag{1}$$

whereω, M, P_m, P_e, D and ΔP are defined as the generator rotor angular speed, inertia, mechanical power, electromagnetic power, damping, and unbalanced power, respectively.

The existing algorithm of unbalanced power for adaptive UFLS is shown as follows:

$$M_{\text{eq}}\frac{df_{\text{coi}}}{dt} = -\Delta P, \tag{2}$$

$$M_{\text{eq}} = \sum_{i=1}^{N} M_j, \tag{3}$$

$$f_{\text{coi}} = \frac{\sum_{i=1}^{N} M_i \cdot f_i}{\sum_{i=1}^{N} M_i}, \tag{4}$$

where M_{eq}, f_{coi} and ΔP are defined as system equivalent inertia, the frequency of the center of inertia (COI) and unbalanced power, respectively.

For the traditional UFLS, its action condition is trigger of threshold value. When the frequency decrease to the first-round action threshold of the UFLS device, a certain proportion of load is shed at the moment t_{shed1}. $t1$ and $t2$ correspond to the moments before and after t_{shed1}, respectively. The interval time between $t1$ and $t2$ is generally within 0.5s. According to equation (2), the following (5) and (6) can be obtained.

$$-\Delta P_{t=t1} = M_{eq}\frac{df_{coi}}{dt}_{t=t1}, \tag{5}$$

$$-\Delta P_{t=t2} = M_{eq}\frac{df_{coi}}{dt}_{t=t2}, \tag{6}$$

where$\Delta P_{t=t1}$, $\Delta P_{t=t2}$ are the unbalanced power at the moments $t1$ and $t2$, respectively.

$$\Delta P_{t=t1} = P_{L,t=t1} + P_{Loss,t=t1} - P_{m,t=t1}, \tag{7}$$

$$\Delta P_{t=t2} = P_{L,t=t2} + P_{Loss,t=t2} - P_{m,t=t2}, \tag{8}$$

where $P_{L,t=t1}$, $P_{m,t=t1}$ and $P_{Loss,t=t1}$ are defined as system load power, transmission loss and mechanical power at the moment $t1$, respectively; and $P_{L,t=t2}$, $P_{m,t=t2}$ and $P_{Loss,t=t2}$ are defined as system load power, transmission loss, and mechanical power at the moment $t2$, respectively.

Subtracting equation (7) and (8), $\left|P_{m,t=t1} - P_{m,t=t2}\right|$ is small due to the inertia limitation of generators, and $\left|P_{Loss,t=t1} - P_{Loss,t=t2}\right|$ is also small because of the characteristics of transmission loss. Therefore, the change amount of mechanical power and transmission loss between $t1$ and $t2$ moments is ignored in the formula (9).

$$M_{eq}\left(\frac{df_{coi}}{dt}_{t=t1} - \frac{df_{coi}}{dt}_{t=t2}\right) = -(P_{L,t=t1} - P_{L,t=t2}), \tag{9}$$

$$M_{eq} = -\frac{(P_{L,t=t1} - P_{L,t=t2})}{\left(\frac{df_{coi}}{dt}_{t=t1} - \frac{df_{coi}}{dt}_{t=t2}\right)}. \tag{10}$$

Since the variables in equation (10) can be measured by WAMS, a method for calculating the real-time inertia of the system on the basis of response information can be acquired. And the power deficit and a centralized UFLS scheme can be further derived.

However, if the system separates into several parts after disturbance, each disconnected subsystem must contain a control center and a complete communication network in order to calculate system inertia M_{eq}. The centralized UFLS scheme is still difficult to implement in disconnected subsystem because the ways of disconnection are unpredictable due to various fault conditions and operation modes. Therefore, a decentralized UFLS scheme on the basis of load information is a better choice for the disconnected subsystem or the area without a control center.

The calculation method of centralized and decentralized unbalanced power is shown in equation (11) and (12), respectively.

$$M_{eq}\frac{df_{coi}}{dt}_{t=ti} = -\Delta P_{t=ti}, \tag{11}$$

$$\sum_{j}^{N} M_{j,eq} \frac{df_j}{dt}_{t=ti} = -\Delta P_{t=ti}, \tag{12}$$

where $\Delta P_{t=ti}$ is the unbalanced power at the moment ti; and $M_{j,eq}$ is the equivalent virtual inertia of the jth load.

Equation (13) can be derived as follows:

$$M_{eq} \frac{df_{coi}}{dt}_{t=ti} = \sum_{j}^{N} M_{j,eq} \frac{df_j}{dt}_{t=ti}. \tag{13}$$

It is supposed that the synchronization stability problem does not occur in the disconnected subsystem. Hence, it can be considered that RoCoF of inertia center $\frac{df_{coi}}{dt}_{t=ti}$ is similar to RoCoF of the jth load $\frac{df_j}{dt}_{t=ti}$.

Then equation (14) is obtained as follows:

$$M_{eq} = \sum_{j}^{N} M_{j,eq} \ (j = 1, 2.....N). \tag{14}$$

The sum of the equivalent virtual inertia of each load in the system is equal to the equivalent inertia of the system. When there are no control centers and reliable communication devices in the system, the equivalent virtual inertia of the jth load can be calculated merely by the load information. Equation (15) is derived as follows:

$$M_{j,eq} = -\frac{(P_{jL,t=t1} - P_{jL,t=t2})}{(\frac{df_j}{dt}_{t=t1} - \frac{df_j}{dt}_{t=t2})}, \tag{15}$$

where $\frac{df_j}{dt}_{t=t1}$ and $\frac{df_j}{dt}_{t=t2}$ are the RoCoF of the jth load at the moments $t1$ and $t2$, respectively; $P_{jL,t=t1}$ and $P_{jL,t=t2}$ are the load power of the jth load at the moments $t1$ and $t2$, respectively.

III. DECENTRALIZED UFLS SCHEME

A. CALCULATION METHOD OF THE POWER DEFICIT

According to equation (2) and the equivalent virtual inertia of the jth load, the unbalanced power of the jth load at the moment $t1$ is defined as follows:

$$\Delta P_{j,t=t1} = -M_{j,\mathrm{eq}} \frac{df_j}{dt}_{t=t1}. \tag{16}$$

The static characteristic of the load is as follows:

$$P_L = P_{L0}(a\frac{U_t}{U_0}^2 + b\frac{U_t}{U_0} + c)(1 + L_{DP}\Delta f), \tag{17}$$

where P_L is the load power in real time;P_{L0} is the stable load power at the rated frequency; U_0 is the initial voltage; a, b and c are the proportion of constant impedance, constant current and constant power in load model, respectively; L_{DP} is the frequency factor; Δf is the offset of frequency.

The power deficit includes two parts: unbalanced power and power shortage caused by voltage offset. When the system is disturbed, the offset of the initial frequency tends to be small, and the change amount of the load power is mainly caused by the voltage offset. The power shortage of the jth load caused by voltage offset is as follows:

$$\varepsilon_{j,t=T} = P_{jL,t=t_0^-} - P_{jL,t=T}, \tag{18}$$

where $P_{jL,t=t_0^-}$ and $P_{jL,t=T}$ are the jth load power at $t = t_0^-$ and $t = T$, respectively. The load information of frequency and power are mainly needed by the proposed method. And $P_{jL,t=t_0^-}$ and $P_{jL,t=T}$ can be acquired in real time according to the measuring device.

Equation (16) is adopted to calculate the unbalanced power at the moment $t1$ of the jth load. To obtain the total power deficit at the moment $t1$, the power shortage caused by voltage offset must be compensated according to equation (18). So the power deficit of the jth load at the moment $t1$ can be estimated according to equations (16) and (18). It is shown as (19).

$$\Delta P_{j,\mathrm{total},t=t1} = -M_{j,\mathrm{eq}} \frac{df_j}{dt}_{t=t1} + \varepsilon_{j,t=t1}. \tag{19}$$

B. ADAPTIVE DECENTRALIZED UFLS SCHEME

When the island system lacks a control center, only the local load information can be utilized to carry out UFLS control. In order to improve the availability of UFLS control, an adaptive decentralized UFLS scheme based on load information is presented in this paper.

A certain proportion of load is shed when the system frequency threshold of UFLS is triggered. On the basis of the load information before and after the 1st round, the equivalent virtual inertia of load is calculated by equation (15). Therefore, the power deficit of each load can be estimated after the 1st round of UFLS by (19). After deducting the load shedding amount of the 1st round, the remaining is the actual remaining power deficit $\Delta P_{\mathrm{shed2}}$. It should be stressed that the startup conditions of 1st round load shedding are set as the same as traditional UFLS schemes to avoid malfunction for the first step.

Then, two basic rounds (2nd round and 3rd round) are set up in the light of $\Delta P_{\mathrm{shed2}}$. Most part of $\Delta P_{\mathrm{shed2}}$ is settled in the 2nd round, which prevents the system frequency from dropping as quickly as possible. A small part of $\Delta P_{\mathrm{shed2}}$ is ordered in the 3rd round, which can reduce the calculation error of the power deficit to a certain extent.

The power deficit is divided into two basic rounds which can bring some advantages. Firstly, the error caused by inertia estimation based on load information can be reduced. More specifically, the error between RoCoF of inertia center and RoCoF of the load is reduced. Secondly, the functions of controllers such as the generator governors are also fully utilized to achieve better frequency stability with less load shedding.

The special round is set to prevent system frequency hover due to other unconsidered factors, and it is independent from the basic rounds movements.

The flowchart of the adaptive decentralized UFLS scheme is shown in Fig. 1.

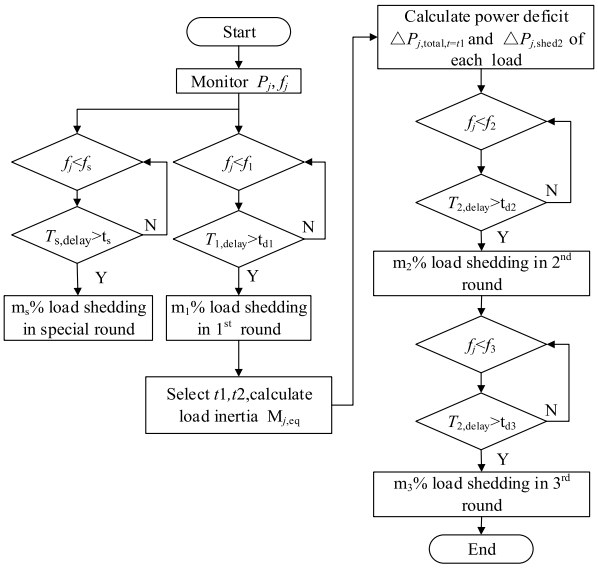

FIGURE 1. Flowchart of decentralized UFLS scheme.

TABLE 1. The decentralized adaptive load shedding scheme.

	I	II	III	IV
Frequency(Hz)	f_1	f_2	f_3	f_s
Delay(s)	t_{d1}	t_{d2}	t_{d3}	t_s
Load shedding (p.u.)	m_1%	m_2%	m_3%	m_s%

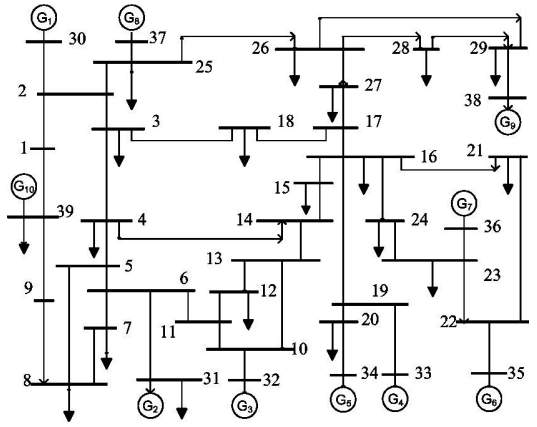

FIGURE 2. Wiring diagram of IEEE 39-bus system.

The decentralized UFLS scheme of this paper is listed in Table 1.

IV. SIMULATION

The simulation is carried out in the IEEE39-bus system. And wiring diagram of IEEE39-bus system is displayed in Fig. 2. To verify the accuracy of the proposed scheme, the following scenarios are simulated.

Table 2 and Table 3 give the information about the generators and load buses in the island grid.

TABLE 2. Power and inertia of each generator.

Generators	Power/p.u	Inertia/s
G4	6.32	57.2
G5	5.08	52.0
G6	6.50	69.6
G7	5.60	52.8
G9	8.30	69.0

TABLE 3. Power of each load.

Load bus	Power /p.u.
15	3.200
16	3.294
20	6.280
21	2.740
23	2.475
24	3.086
26	1.390
27	2.810
28	2.060
29	2.835

TABLE 4. Equivalent virtual inertia of each load bus in scenario A.

Load bus	Inertia/s
16	19.59
20	27.64
21	18.39
23	18.48
24	18.06
26	8.94
27	18.88
28	17.50
29	24.54

The parameters of the decentralized UFLS scheme in this paper are set as follows:

1) 1st round: $f_1 = 49\text{Hz}$, $t_{d1} = 0.2\text{s}$, $m_1\% = 5\%$;

2) 2nd round: $f_2 = 48.6Hz$, $t_{d2} = 0.2\text{s}$, $m_2\% = \Delta P_{shed2} \times k_2$, where $k_2 = 0.8$;

3) 3rd round: $f_3 = 48.2Hz$, $t_{d3} = 0.2\text{s}$, $m_3\% = \Delta P_{shed2} \times k_3$, where $k_3 = 0.1$;

4) Special round: $f_s = 49Hz$, t_s=10s, $m_s\% = 5\%$;

A. SCENARIO A

The disturbance is set at 0.2s, generators G5 and G6 are tripped, at the same time, the lines 15-16-17-18 and 25-26 are disconnected. The remaining generators consist of G4G7 and G9 on the island. An island is established on the right side of IEEE39-bus system. The load buses include 16, 20, 21, 23, 24, 26, 27, 28 and 29. The generator model adopts the constant E'_q model with voltage regulator and governor. The load model adopts a 70% constant impedance and a 30% constant power model.

Frequency threshold is triggered in the 1st round at the moment 2.07s. And 5% load is shed at the moment 2.27s. In this scenario, $t1$ and $t2$ are chosen as 2.07s and 2.47s. According to equation (15), the equivalent virtual inertia of each load is obtained. Calculated inertia is listed in Table 4.

The actual inertia of the island system is 179s after the disturbance occurs. It is supposed that the island has no control centers, the real-time change of inertia or even the frequency of COI are difficult to obtain. Thus, the traditional adaptive UFLS schemes will be affected.

According to Table 4, the equivalent virtual inertia of each load calculated with the proposed method is added to 172.02s, which is close to the actual value 179s.

The mechanical power of the system after the disturbance is 20.22p.u.. The initial load power is 26.97p.u.. And the actual power deficit of the system can be derived which is $\Delta P_{t=t_0^-} = 25.03\%$.

$\Delta P_{j,\text{total},t=t1}$ of each load is acquired according to Table 4 and equation (19). The results in proportion are shown in Fig. 3, and listed in per unit in Table 5.

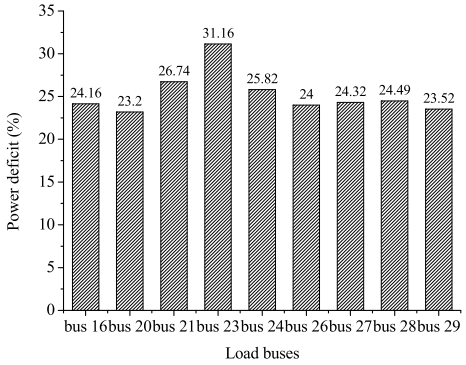

FIGURE 3. Power deficit of each load in scenario A in proportion.

TABLE 5. power deficit of each load in scenario A in per unit.

Load bus	Power deficit /p.u.
16	0.796
20	1.457
21	0.733
23	0.771
24	0.797
26	0.334
27	0.684
28	0.505
29	0.667

$\Delta P_{\text{cal},t=t1}$ is defined as the estimated power deficit of the system. And it can be derived from the power deficit of each load:

$$\Delta P_{cal,t=t1} = \frac{\sum_{j=1}^{N} \Delta P_{j,\text{total},t=t1}}{\sum_{j=1}^{N} P_{j,t=t_0^-}}. \tag{20}$$

It can be concluded from Fig. 3 that the estimated power deficit of each load is inconsistent. But the total estimated power deficit of the system is $\Delta P_{cal,t=t1} = 25.27\%$, which is similar to the actual value $\Delta P_{t=t_0^-} = 25.03\%$.

Load shedding results are shown in Fig. 4. Among them, schemes (1), (2), (3) are traditional UFLS schemes which are

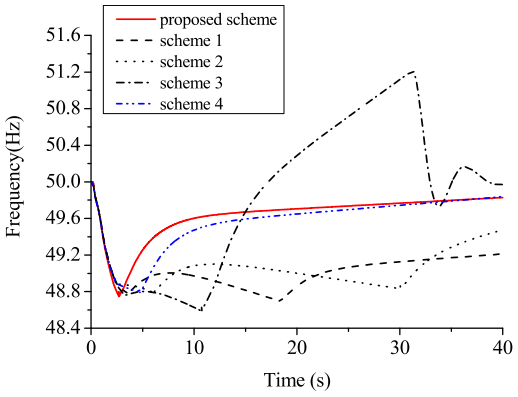

FIGURE 4. Different load shedding schemes in scenario A.

TABLE 6. The action time and load shedding amount of each round in scenario A.

	I	II	III	IV	V	VI
Scheme 1	2.27s 7%	3.47s 7%	- -	- -	- -	18.4s 5%
Scheme 2	2.27s 10%	6.05s 8%	- -	- -	- -	30.05s 5%
Scheme 3	2.27s 5%	3.15s 6%	10.73s 10%	- -	- -	10.07s 5%
Scheme 4	2.27s 9%	4.7s 11%	- -	- -	- -	- -

detailed in the Appendix. Scheme 4 is proposed in [15]. The action time and load shedding amount of each round are listed in Table 6.

The lowest frequency curves of load buses on the island of different control schemes are shown in Fig. 4. Under the premise of no synchronization stability problem, the frequency changes at the load buses on the island are basically the same.

As for the traditional schemes, the frequency of scheme 1 and scheme 2 cannot be recovered in a short time. Although the frequency of scheme 3 can be restored, overshoot of frequency will be caused by over-shedding of the load. Compared to the proposed scheme, scheme 4 requires longer time in the control process.

As can be seen from Table 6, the starting time of the 1st round in different schemes are the same. However, due to the different load shedding amount in different schemes, the starting time of the 2nd round in different schemes are different. Similarly, different starting time of each subsequent round are resulted by different load shedding amount of the 2nd round. As a consequence, different control effects are produced.

From the comparison results, the stronger recovery ability of frequency and the shorter restore time are realized in the proposed scheme, and the performance of UFLS control is improved in the same disturbance scenario.

B. SCENARIO B

The disturbance is set at 0.2s, generators G4 and G5 are tripped, at the same time, the lines 16-17, and 14-15 are disconnected. The load buses include 15, 16, 20, 21, 23, and 24

TABLE 7. Equivalent virtual inertia of each load bus in scenario B.

Load bus	Inertia/s
15	17.28
16	18.59
20	22.83
21	17.75
23	22.03
24	16.78

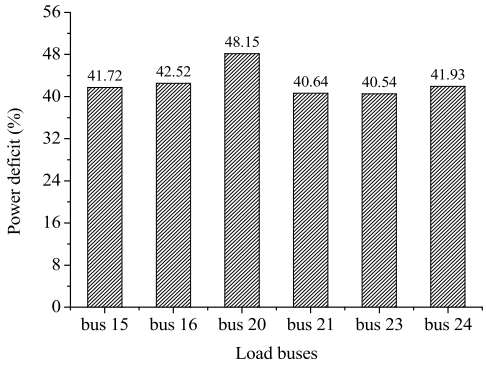

FIGURE 5. power deficit of each load in scenario B in proportion.

TABLE 8. power deficit of each load in scenario B in per unit.

Load bus	Power deficit /p.u.
15	1.335
16	1.401
20	3.024
21	1.114
23	1.003
24	1.294

on the island. The remaining generators consist of G6 and G7 on the island. The load model adopts a 60% constant impedance, a 20% constant current and a 20% constant power model. The remaining conditions are the same as scenario A.

The equivalent virtual inertia of each load can be calculated according to equation (15), which is listed in Table 7.

The island inertia was 231.6s before the disturbance which drops to 122.4s when the units G4 and G5 are tripped simultaneously. According to Table 7, the sum of decentralized equivalent virtual inertia is 115.26s, which is close to the actual value.

According to the set disturbance, the mechanical power of the system after the disturbance is $P_{m,t=t_0^+} = 12.10$p.u.. The initial load power is $P_{L,t=t_0^-} = 21.075$p.u.. And the actual power deficit of the system is acquired which is $\Delta P_{t=t_0^-} = 42.59\%$.

$\Delta P_{j,\text{total},t=t1}$ of each load is obtained according to Table 7 and equation (19). Results in proportion are shown in Fig. 5, and listed in per unit in Table 8.

Total estimated power deficit of the system is $\Delta P_{cal,t=t1} = 42.58\%$ on the basis of equation (20), which is approaching to actual value $\Delta P_{t=t_0^-} = 42.59\%$.

The load shedding results are shown in Fig. 6. In scenario B, the traditional UFLS schemes (1), (2), (3) are unable to restore the frequency stability in a short time, This is

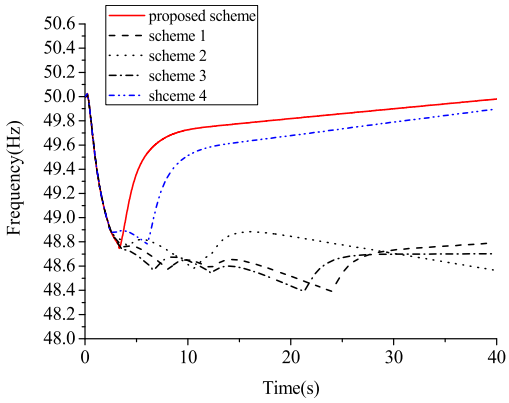

FIGURE 6. Different load shedding schemes in scenario B.

TABLE 9. Power of each load in scenario C.

Load bus	Power /p.u.
15	7.075
16	9.000
20	1.500
21	1.200
23	1.000
24	1.300

because after the disturbance, the proportion of the power deficit is relatively large, and the traditional schemes need longer time and more rounds to restore the frequency stability. Compared with the traditional schemes, the proposed scheme in this paper can adaptively calculate the power deficit of each load and carry out corresponding decentralized control, so that the system frequency can be recovered to the required range quickly.

From the simulation in scenario A and scenario B, it can be seen that in the absence of the information of centralized control, the proposed scheme merely utilize the load response information to estimate the power deficit of each load. Although there is a certain deviation in the calculation of the power deficit for each load, the estimated value of the power deficit for the system is similar to the actual value. As a result, the estimated power deficit of each load provides a reference for load shedding control of UFLS, and it enhances the reliability and accuracy of the decentralized UFLS scheme.

C. SCENARIO C

The disturbance and parameters are set as the same as scenario B, but the load distribution is changed in scenario C. Specifically, the loads are mainly concentrated in the northwest corner of the island, and power of each load is as listed in Table 9.

The equivalent virtual inertia and the power deficit of each load can be estimated according to the proposed method, which are listed in Table 10.

The equivalent virtual inertia of the island is added to 117.95s according to Table 10, which is approaching to the actual value 122.4s. And the total estimated power deficit of

TABLE 10. Equivalent virtual inertia and the power deficit of each load bus in scenario C.

Load bus	Inertia/s	Power deficit/%
15	36.89	45.26
16	50.46	45.86
20	6.94	50.47
21	7.62	44.47
23	8.99	45.91
24	7.05	45.54

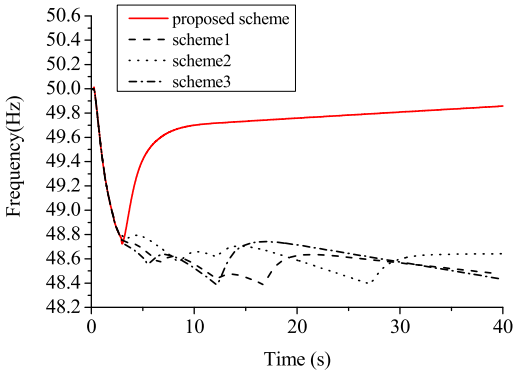

FIGURE 7. Different load shedding schemes in scenario C.

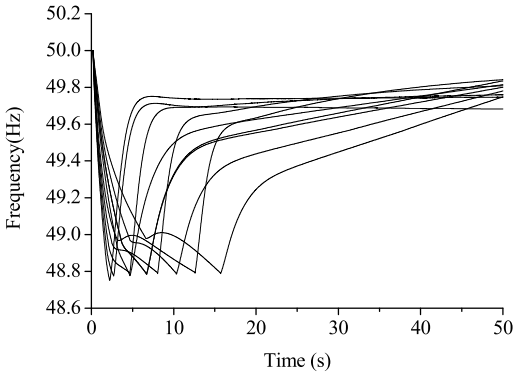

FIGURE 8. The proposed scheme in different operating points.

the system is 46.25% on the basis on equation (20), which is close to actual value 42.59%. In additional, the load shedding results are shown as Fig. 7.

As can be seen from Fig. 7, the validity of the proposed scheme can also be verified where loads are not so evenly dispersed across the network. As a matter of fact, the proposed scheme can perform effectively under the premise of no transient stability problems.

D. SCENARIO D

The parameters and conditions of scenario D are set based on scenario B but remaining generators G5, G6 and G7 on the island. In scenario D, the output of generation is changed to verify the availability of the proposed scheme in different operating points. To be specific, the power generation of G5 increases from 100MW to 550MW with 50MW increment for each operating mode. Meanwhile, G6 and G7 remain unchanged. The 10 load shedding results are shown in Fig.8.

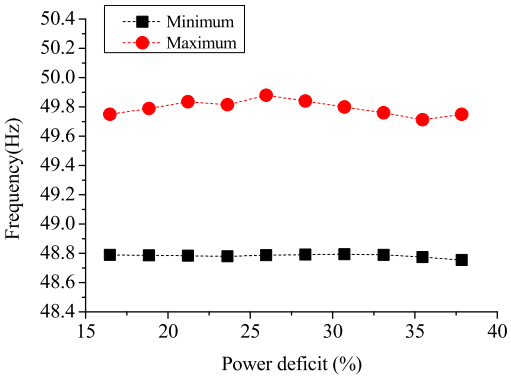

FIGURE 9. Minimum and maximum frequency in different operating points.

TABLE 11. A general-round-by-round load shedding scheme 1.

	I	II	III	IV	V	VI
Frequency(Hz)	49	48.8	48.6	48.4	48.2	49
Delay(s)	0.2	0.2	0.2	0.2	0.2	10
Load shedding (%)	7	7	8	8	12	5

It can be concluded from Fig.8 that the proposed load shedding method has good frequency recovery ability in different operating points. The minimum frequency and the maximum frequency of each operating point are shown in Fig. 9.

In Fig. 9, the abscissa indicates the power deficit ratio in each operating point. Power deficit changes in the range of 16.47% to 37.84% according to the changes in power generation in scenario D. As is shown in Fig. 8 and Fig. 9, the minimum frequency is basically the same due to the same trigger condition. And the maximum frequency of different operating points can be restored to about 49.8Hz by the proposed scheme. As can be seen from load shedding results, the applicability and availability of the proposed scheme in different operating points are further demonstrated.

V. CONCLUSION

In this paper, a decentralized UFLS scheme on the basis of load information is proposed. To begin with, the equivalent virtual inertia and the power deficit of each load can be estimated merely by load information. Then, an independent decentralized adaptive UFLS relay control method is presented based on the power deficit of each load. Governor and other controllers are fully taken into account in the proposed scheme. It can be seen from the simulation results that the proposed UFLS scheme has excellent adaptability and performance in multiple scenarios. A better frequency recovery effect is obtained with a smaller load shedding amount compared with the traditional UFLS. Besides, the proposed method is easy to implement and the required information is also easy to achieve. As a result, the feasibility and applicability of decentralized UFLS control are improved effectively.

TABLE 12. A general-round-by-round load shedding scheme 2.

	I	II	III	IV	V	VI
Frequency(Hz)	49	48.8	48.6	48.4	48.2	49
Delay(s)	0.2	0.2	0.2	0.2	0.2	10
Load shedding (%)	10	8	8	6	10	5

TABLE 13. A general-round-by-round load shedding scheme 3.

	I	II	III	IV	V	VI
Frequency(Hz)	49	48.8	48.6	48.4	48.2	49
Delay(s)	0.2	0.2	0.2	0.2	0.2	10
Load shedding (%)	5	6	10	8	12	5

APPENDIX

See Tables 11–13.

REFERENCES

[1] P. Kundur *et al.*, "Definition and classification of power system stability IEEE/CIGRE joint task force on stability terms and definitions," *IEEE Trans. Power Syst.*, vol. 19, no. 2, pp. 1387–1401, Aug. 2004.
[2] *IEEE Guide for Abnormal Frequency Protection for Power Generating Plants*, IEEE Standard C37.106-2003, 2004, pp. 1–34.
[3] *IEEE Guide for the Application of Protective Relays Used for Abnormal Frequency Load Shedding and Restoration*, IEEE Standard C37.117-2007, 2007, pp. 1–55.
[4] J. Tang, J. Liu, F. Ponci, and A. Monti, "Adaptive load shedding based on combined frequency and voltage stability assessment using synchrophasor measurements," *IEEE Trans. Power Syst.*, vol. 28, no. 2, pp. 2035–2047, May 2013.
[5] J. De La Ree, V. Centeno, J. S. Thorp, and A. G. Phadke, "Synchronized phasor measurement applications in power systems," *IEEE Trans. Smart Grid*, vol. 1, no. 1, pp. 20–27, Jun. 2010.
[6] W. Yang, L. Wenyuan, and L. Jiping, "Reliability analysis of wide-area measurement system," *IEEE Trans. Power Del.*, vol. 25, no. 3, pp. 1483–1491, Jul. 2010.
[7] P. M. Anderson and M. Mirheydar, "An adaptive method for setting underfrequency load shedding relays," *IEEE Trans. Power Syst.*, vol. 7, no. 2, pp. 647–653, May 1992.
[8] L. Sigrist, "A UFLS scheme for small isolated power systems using rate-of-change of frequency," *IEEE Trans. Power Syst.*, vol. 30, no. 4, pp. 2192–2193, Jul. 2015.
[9] L. Shun, L. Qingfen, and L. Dichen, "WAMS based dynamic optimization of adaptive under-frequency load shedding," *Power Syst. Protection Control*, vol. 44, no. 13, pp. 48–54, 2016.
[10] U. Rudez, J. Bogovic, and R. Mihalic, "Probability-based approach for parametrisation of traditional underfrequency load-shedding schemes," *IET Gener., Transmiss. Distrib.*, vol. 9, no. 16, pp. 2625–2632, 2015.
[11] U. Rudez and R. Mihalic, "WAMS-based underfrequency load shedding with short-term frequency prediction," *IEEE Trans. Power Del.*, vol. 31, no. 4, pp. 1912–1920, Aug. 2016.
[12] J. Jallad, S. Mekhilef, J. A. Laghari, and H. Mokhlis, "Improved UFLS with consideration of power deficit during shedding process and flexible load selection," *IET Renew. Power Gener.*, vol. 12, no. 5, pp. 565–575, 2018.
[13] K. Mehrabi, S. Afsharnia, and S. Golshannavaz, "Toward a wide-area load shedding scheme: Adaptive determination of frequency threshold and shed load values," *Int. Trans. Elect. Energy Syst.*, vol. 28, no. 1, p. e2470, 2018.
[14] K. Mehrabi, S. Golshannavaz, and S. Afsharnia, "An improved adaptive wide-area load shedding scheme for voltage and frequency stability of power systems," *Energy Syst.*, pp. 1–22, May 2018. doi: 10.1007/s12667-018-0293-9.
[15] S. Li, F. Tang, Q. Liao, and Y. Shao, "Adaptive under-frequency load shedding scheme in system integrated with high wind power penetration: Impacts and improvements," *Energies*, vol. 10, no. 9, pp. 1331–1347, 2017.
[16] U. Rudez and R. Mihalic, "A novel approach to underfrequency load shedding," *Electr. Power Syst. Res.*, vol. 81, no. 2, pp. 636–643, 2011.
[17] U. Rudez and R. Mihalic, "Predictive underfrequency load shedding scheme for islanded power systems with renewable generation," *Elect. Power Syst. Res.*, vol. 126, pp. 21–28, Sep. 2015.
[18] D. Y. Yang, G. W. Cai, and Y. T. Jiang, "Centralized adaptive under frequency load shedding schemes for smart grid using synchronous phase measurement unit," *J. Elect. Eng. Technol.*, vol. 8, no. 3, pp. 446–452, 2013.
[19] A. M.-Bolhasan, H. Seyedi, B. M.-Ivatloo, S. Abapour, and S. Ghasemzadeh, "Modified centralized ROCOF based load shedding scheme in an islanded distribution network," *Int. J. Elect. Power Energy Syst.*, vol. 62, pp. 806–815, Nov. 2014.
[20] W. Gu *et al.*, "Adaptive decentralized under-frequency load shedding for islanded smart distribution networks," *IEEE Trans. Sustain. Energy*, vol. 5, no. 3, pp. 886–895, Jul. 2014.
[21] W. Gu, W. Liu, C. Shen, and Z. Wu, "Multi-stage underfrequency load shedding for islanded microgrid with equivalent inertia constant analysis," *Int. J. Elect. Power Energy Syst.*, vol. 46, no. 1, pp. 36–39, 2013.

PEICAN HE received the B.Eng. degree in electrical engineering from Fuzhou University, China, in 2017, where he is currently pursuing the master's degree. His research interest includes power systems stability and control.

BUYING WEN received the B.Eng., master's, and Ph.D. degrees in electrical engineering from Fuzhou University, China, in 1991, 1998, and 2006, respectively. He was a Visiting Scholar with Shanghai Jiaotong University, in 2001. His research interests include power market and wind power operation technology.

HUAIYUAN WANG received the B.Eng. and Ph.D. degrees in electrical engineering from Xi'an Jiaotong University, China, in 2010 and 2016, respectively. His research interests include power systems modeling, and power systems stability and control.